Biophysical Journal
Article

Biophysical Society

Transcriptional Bursts in a Nonequilibrium Model for Gene Regulation by Supercoiling

Marco Ancona,[1,*] Alessandro Bentivoglio,[1] Chris A. Brackley,[1] Giuseppe Gonnella,[2] and Davide Marenduzzo[1]
[1]SUPA, School of Physics and Astronomy, University of Edinburgh, Edinburgh, United Kingdom and [2]Dipartimento di Fisica, INFN, Università degli Studi di Bari Aldo Moro, Sezione di Bari, Bari, Italy

ABSTRACT We analyze transcriptional bursting within a stochastic nonequilibrium model, which accounts for the coupling between the dynamics of DNA supercoiling and gene transcription. We find a clear signature of bursty transcription when there is a separation between the timescales of transcription initiation and supercoiling dissipation (the latter may either be diffusive or mediated by topological enzymes, such as type I or type II topoisomerases). In multigenic DNA domains, we observe either bursty transcription or transcription waves; the type of behavior can be selected for by controlling gene activity and orientation. In the bursty phase, the statistics of supercoiling fluctuations at the promoter are markedly non-Gaussian.

INTRODUCTION

Transcription, the mechanism through which DNA is read by a polymerase to create a messenger RNA, is a crucial process in living cells, and its regulation is an important determinant of cell function (1). The dynamics of transcription are inherently stochastic because its initiation requires an RNA polymerase (RNAP) and associated cofactors to bind at the promoter of a gene (2). Not only can the copy numbers of RNAPs and transcription factors be low, but the mechanism through which they find their specific binding sites (a combination of three-dimensional diffusion through the nucleoplasm or cytoplasm and one-dimensional diffusion along the genome (3,4)) leads to a broad distribution of search times. As a consequence, transcription initiation is a rare event with rates of the order of inverse hours in mammals (5), whereas in bacteria, tens of minutes may elapse between successive initiation events at the same promoter (6).

An intriguing feature of transcription as a stochastic process is that it is often "bursty." This means that when recording transcription events for a given gene in a given cell, one observes clusters of closely spaced events separated by longer dormant periods in which the gene is silent, and the distribution of interval times is non-Poissonian. Transcription bursts are common to both bacterial and eukaryotic cells; this phenomenon is thought to provide a potential basis for the variability in behavior, which is observed in genetically identical cells within the same environment (2). Bursting may therefore play a key role in the pathway through which a cell can spontaneously break symmetry, for instance to choose its fate early in development in higher eukaryotes (7).

From a general point of view, a dynamical system yields bursty behavior when there is intermittent switching between states with high and low activity (8,9). But what is the biophysical mechanism underlying such intermittency? Several possibilities have been proposed in the literature, and they may differ in different organisms. In mammals, proposed mechanisms for bursting are typically gene specific (10); cycles of higher transcription activity may be due to chromatin remodeling (11) or to the action of *cis*-regulatory DNA elements (10). In both cases, refractory periods during which genes are silent last for hours. In bacteria, refractory timescales only span tens of minutes, and other scenarios may be more relevant. For instance, pausing of an RNAP along a gene may lead to the formation of a queue of multiple RNAPs behind it, producing bursts of transcripts (12,13). This mechanism requires that the gene in question is highly expressed so that multiple polymerases can be recruited to its promoter within minutes. Recently, a set of experiments (14) has demonstrated that transcriptional bursts in DNA plasmids in vitro are associated with DNA supercoiling (15), which is the extent of over- or underwinding of the two strands in a DNA double helix. Specifically, it was shown that the buildup of positive supercoiling (DNA overtwisting) stalls transcription, and the addition of gyrase

Submitted March 22, 2019, and accepted for publication April 11, 2019.
*Correspondence: mar.ancona92@gmail.com
Editor: Andrew Spakowitz.
https://doi.org/10.1016/j.bpj.2019.04.023

(which relaxes this supercoiling) leads to transcriptional bursts (14). The conclusions of this work are consistent with the hypothesis in the earlier rate-based theoretical model in (9), which suggested that the timescales observed in bacterial bursts are compatible with supercoiling-dependent initiation.

Here, we consider a stochastic model, which couples the dynamics of supercoiling and transcription in DNA (first introduced in (16)) and ask whether, and under which conditions, supercoiling may lead to transcriptional bursts. Our main result is that supercoiling can induce bursts in a wide range of parameter space. Perhaps surprisingly, bursts occur only when the overall transcriptional rate is low and are absent when it is high. When gene density is low (e.g., if we model a single gene), significant bursting is primarily found in the presence of topological enzymes, which relax supercoiling at a fixed rate. For higher gene density, highly significant bursts can also arise in the absence of topoisomerases through the action of a self-organized nonequilibrium regulatory network mediated by supercoiling. Intriguingly, this same pathway can also generate transcription waves and upregulate divergent transcription, both of which eventually disrupt the bursty behavior. A final key finding is that bursting leaves a detectable signature in the distribution of supercoiling at the promoter; it leads to a nonnormal distribution and the appearance of a singularity or small peak in the tails of the distribution. Observation of such signatures may be an aim of future experiments, along the lines of existing ones, performed either in vitro (14) or in vivo (17,18).

MATERIALS AND METHODS

Model

The key dynamical variable in our model is a one-dimensional scalar field $\sigma(x,t)$, which denotes the local supercoiling density at a point x on the DNA. This is the local analog of the global supercoiling density, defined as $(Lk-Lk_0)/Lk_0$, where Lk is the linking number of a DNA molecule (which can be decomposed into twist and writhe (15)) and Lk_0 is the linking number of a torsionally relaxed B-DNA (i.e., 1 for every 10.5 base pairs [bps]). Because both Lk and Lk_0 can be defined for a segment of the DNA molecule, an analogous formula can be used to define σ locally; doing this is analogous to approximating writhe with a local field (19). The dynamics are then described in continuous space by

$$\frac{\partial\sigma(x,t)}{\partial t} = \frac{\partial}{\partial x}\left[D\frac{\partial}{\partial x}\sigma(x,t) - J_{\mathrm{tr}}(x,t)\right] - k_{\mathrm{topo}}\sigma(x,t), \quad (1)$$

where the three terms on the right-hand side represent diffusion of supercoiling, supercoiling flux generated by transcription, and supercoiling dissipation due to topological enzymes. Below, we will discuss each term in turn. Although we have written Eq. 1 as continuous in space, we solve it on a lattice of length $L = 15$ kbp with spacing $\Delta x = 15$ bp (which is approximately the footprint size of an RNAP).

If we consider a closed DNA loop, then in the absence of topological enzymes, the total level of supercoiling is conserved (it is a topological invariant of the system). Therefore, we require that supercoiling obeys "model B" (conserved) dynamics (20). Further, the free-energy density of supercoiling (twist and writhe) f is, to a good approximation, quadratic in the supercoiling density (15,16); so the chemical potential $(\partial f/\partial\sigma)$ is linear in σ. Because the flux in model B dynamics is proportional to the gradient of the chemical potential, this results in a diffusion equation (when the mobility is constant) (16), giving the first term on the right of Eq. 1. Single-molecule measurements of the dynamics of plectonemic supercoils in vitro (21) and studies of transcription in vivo (22) are also consistent with a diffusive dynamics for supercoiling.

The second term in Eq. 1 represents supercoiling fluxes due to transcription. Through this term, we couple the supercoiling dynamics to stochastic transcriptional kinetics, where each of N RNAPs can bind at the promoters of n genes (each of size $\lambda = 66\Delta x \approx 1000$ bp) located at lattice positions y_j, $j = 1, \ldots, n$. Transcription initiates stochastically when an inactive RNAP binds at gene j with rate $k_{\mathrm{in},\,j}$. The RNAP then elongates with velocity v (positive or negative depending on the direction of transcription) such that at a time t_i after initiating it is located at position $x_i(t_i) = y_j + vt_i$ (where the index i labels the RNAP). Transcription terminates (and the promoter becomes again available for initiation) once the RNAP reaches the end of a gene. The total flux is then given by

$$J_{\mathrm{tr}}(x,t) = \sum_{i=1}^{N} J_i(t_i)\delta(x - x_i(t_i))\eta_i(t), \quad (2)$$

where the sum is over all RNAPs, $J_i(t_i)$ is the flux generated by RNAP i, and the function $\eta_i(t)$ represents its state, taking a value of zero if it is unbound and one if it is actively transcribing. The initiation dynamics is coupled back to the supercoiling by making $k_{\mathrm{in},\,j}$ a function of the supercoiling at the promoter,

$$k_{\mathrm{in},j}(t) = k_0 \max\{1 - \alpha\sigma(x_j,t), 0\}, \quad (3)$$

where α is a coupling parameter (it represents the sensitivity of RNAP-DNA binding to the level of supercoiling).

According to the twin supercoiling domains model (23), a moving RNAP generates a supercoiling flux if its rotation is hindered because as the enzyme progresses, the DNA has to locally unwind. (The rotational drag on the RNAP in vivo is likely to be large in view of its size and of its interactions with other macromolecules). As a result, positive supercoiling is generated in front of the RNAP and negative supercoiling behind. More specifically, as the RNAP moves, all the DNA twist in front of it (minus any rotation of the RNAP if present) is pushed forward. This reasoning suggests that the flux generated will depend on the level of twist ahead of the RNAP, which might in principle vary (12). However, to obtain a tractable model, we assume the flux to be constant. In practice, this approximation is likely good because DNA can only support small levels of twist before writhing (24).

A final complication is that the diffusion of supercoils through the RNAP also requires its rotation; hence, we expect this effect to be small. We could prohibit flux through the RNAPs by introducing no-flux boundary conditions at the points x_i, but an alternative, which yields a more tractable model, is to instead ramp up the flux as transcription progresses; to do this we set

$$J_i(t_i) = J_0\left(1 + \frac{|v|\,t_i}{\Delta x}\right). \quad (4)$$

The sign of J_0 depends on the direction of transcription. Any residual net diffusive leak only plays a minor role because it is small compared to J_0. (Additionally, a small leak of supercoiling may not be unrealistic even for a polymerase acting as a topological barrier for twist, if the region of DNA containing it writhes in three dimensions). In what follows, we define $\overline{J} = J_0[1 + \lambda/(2\Delta x)]$; this is a useful quantity because it is the average value of the supercoiling flux generated during a transcription event.

The third term on the right of Eq. 1 represents the loss of supercoiling due to the action of topoisomerases (such as, e.g., topoI, topoII, gyrase). This is

introduced in the model in a minimal way as a first-order reaction where both positive and negative supercoiling relax at the same rate k_{topo}. In general, this term does not conserve the total supercoiling; however, here, we start with a uniform initial condition $\sigma(x, t = 0) \equiv \sigma_0$, where $\sigma_0 = 0$, so in this case, the total supercoiling is conserved.

This model was first described in (16). In that work, it was found that by increasing the ratio $\bar{J}/D$, there is a crossover from a relaxed regime in which transcription is virtually Poissonian to a supercoiling-regulated regime in which transcription of neighboring genes is highly correlated. In this work, we examine under what conditions the coupling between supercoiling and transcription can lead to bursty dynamics.

Key model quantities and parameter values

Key quantities that control the model behavior are the ratios $\bar{J}/D$ and k_{topo}/k_0. In the results section below, we will explore the ability of the model to exhibit bursty behavior at different points within the $\bar{J}/D$–k_{topo}/k_0 parameter space for different gene arrangement cases. Although the values that these quantities have in vivo have not yet been well characterized experimentally, here, we discuss what ranges of values might be relevant based on available evidence. For our simulations, we vary several parameters to get an understanding of how such a system might behave under different conditions.

The diffusion constant for supercoiling is difficult to measure, not least because one would expect very different values for twist and writhe. Intuitively, one would expect twist to diffuse very quickly (12), whereas writhe diffusion would be much slower because it requires more global DNA rearrangements. Also, it has been shown that DNA is unable to support much deviation of twist from its relaxed state: the theory in (24) (and the references therein) indicate that it will writhe if the supercoiling density exceeds 0.01. This suggests that the slower diffusion of writhe will dominate the dynamics. Single-molecule experiments presented in (21), which measured the motion of plectonemes in a stretched DNA molecule, indeed obtained a relatively small diffusion coefficient, with a value significantly less than 1 kbp^2/s (see Fig. 3 *F* in (21)). Specifically, when a DNA molecule is subjected to tensions of less than 1–2 pN, plectoneme diffusivity is at most ~0.1 kbp^2/s. Taking this value and a typical size for a bacterial gene of $\lambda \approx 1$ kbp, the time it takes for supercoiling to diffuse away from the promoter after transcription terminates is $\lambda^2/2D \approx 5$ s. In vivo, macromolecular crowding is likely to further slow down writhe/supercoiling diffusion, so for our simulations, we consider values for D that are between ~4 and ~40 times smaller than the value quoted above. Specifically, we consider $D \approx 2.25 \times 10^{-2}$ kbp^2/s in Fig. 1 and $D \approx 2.25 \times 10^{-3}$ kbp^2/s in other figures. Both values allow the supercoiling generated during transcription of a gene to dissipate in at most minutes after transcription termination (the smaller value was used for the more systematic analyses because it enables more efficient simulations using a larger value for the time step).

The typical RNAP velocity in bacteria is 100 bp/s (1), so that the time taken to transcribe a $\lambda = 1$ kbp gene is $\tau \sim \lambda / \nu \sim 10$ s. Then, through dimensional analysis, we expect an order-of-magnitude estimate for the $\bar{J}$ to be $\sim \lambda^2 / \tau$ or $\nu\lambda \sim 0.1$ kbp^2/s; notably, this is the same order of magnitude as D. Thus, in our simulations, we explore a range of values for $\bar{J}/D$, which is typically between 0.34 and 3.4.

Turning now to the dynamics of transcription initiation, measured RNAP initiation rates can vary widely, and typical values are in the range 1 s^{-1} to 1 h^{-1} are observed (see (16,25–27)). Likewise, the number of RNAPs has a large variability. For example, in the bacteria *Escherichia coli*, there are an estimated 1000–10,000 RNAPs per cell (28) and ~5000 genes. To reflect this ratio, we take one RNAP per gene in our simulations unless otherwise stated (see Fig. S4). The rate of topoisomerase action in vivo is equally difficult to estimate. Reference (29) counts ~500 topoisomerase I per cell in *E. coli*. Assuming that approximately half the enzymes are bound and that there are two genomes per cell on average, we arrive at ~100 topoisomerase proteins bound per genome or 0.02 per gene. Assuming additionally that each enzyme can on average relax 1–10 supercoils per second (30) and that the baseline bacterial supercoiling is equal to −0.05, we get $k_{topo} \approx 0.005$–0.05 s^{-1}. We note this rough estimate is within the physiological value of the baseline transcriptional rate (in our simulations, k_0). Because of this and because the values of k_{topo} and k_0 are not known accurately, in our simulations, we have systematically varied their ratio k_{topo}/k_0 between 0 and 1.4. (Specifically we set $k_0 = 0.001$ s^{-1} and varied k_{topo}.) In this way, we can examine all possible scenarios concerning the balance between initiation and topoisomerase relaxation rates.

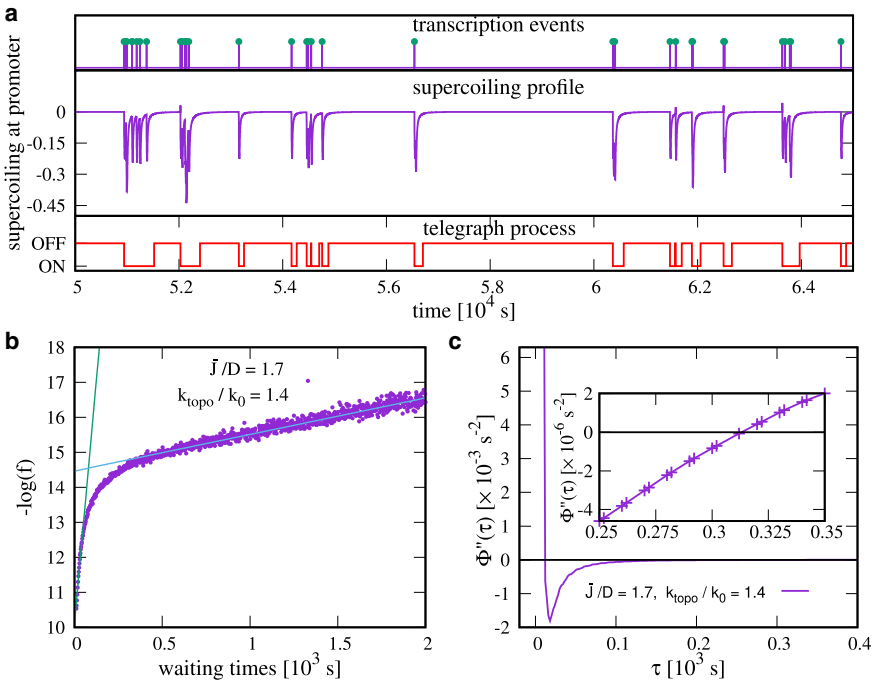

FIGURE 1 Transcriptional bursts and the sequence-size function (ssf). (*a*) A time series for a simulation with $\bar{J}/D = 1.7$, $k_{topo}/k_0 = 1.4$., is shown. Transcription events (*top*) are often grouped in bursts. Transcription initiation depends on the level of supercoiling at the gene promoter (*middle*). The state of the system (*bottom*) is defined as OFF if $\sigma_p \geq (1 - (k_0\tau_2)^{-1})/\alpha$ and ON otherwise. (*b*) The negative logarithm of the pdf of waiting times is shown. The existence of two linear regions characterizes the dynamics as bursty. (*c*) The second derivative of the ssf is shown: the existence of roots at τ_1 and τ_2 demonstrates the presence of two timescales. The inset shows the zoom of the intersection of this second derivative with the x axis close to τ_2. To see this figure in color, go online.

To determine whether supercoiling can affect RNAP initiation at a promoter, we need to consider the time it takes for supercoiling generated by a previous transcription event to diffuse away and the typical initiation rate ($k_{\text{in},\,j}$ in our model). In (16), a mean field model was used to estimate the extent of residual supercoiling at the promoter, and this was given by

$$|\sigma_p| \simeq \frac{\overline{J}}{2D} k_0 \tau. \tag{5}$$

If this quantity is larger than α^{-1} (see Eq. 3 for the definition of α), then supercoiling can indeed increase the rate at which RNAP binds the promoter, leading to a positive feedback. Experiments in bacterial genes suggest that a supercoiling density of $\sigma_p \leq -0.01$ is sufficient to enhance RNAP binding (see (16,31,32)), so in our simulations, we have set $\alpha = 100$. These considerations explain why $\overline{J}/D$ and $k_0 n \tau$ are key dimensionless quantities in our model.

In what follows, we give parameter values either in physical units or in terms of dimensionless ratios. When required, the physical values of all parameters can be reconstructed by referring back to this section. As noted above, to solve Eq. 1 numerically, we discretize space into a lattice with 15-bp spacing; we discretize time into steps of between 0.1 and 1 s, chosen to balance efficiency and numerical stability (which depends on the other parameters).

The sequence-size function

A classic model to describe transcriptional bursting is the interrupted Poisson process (33) (see Supporting Materials and Methods, Section SII), which describes transitions between an active (ON) and an inactive (OFF) state with Poissonian rates k_{ON} and k_{OFF}, as in a random telegraph process (8), together with transcription at a constant rate k_i while the system is in the ON state. The process can be characterized by the probability distribution function (pdf) $f(t)$ of waiting times, the time intervals between two consecutive transcriptional events, which is given by a double exponential (33), where the two characteristic times are related to the interval between transcriptions in a single burst and the interval between two consecutive bursts (see Eqs. S10–S13).

To determine whether our system is bursty for a given set of parameters ($\overline{J}/D$ and k_{topo}/k_0), we measure the distribution $f(t)$. We then analyze the so-called sequence-size function (ssf) (33,34), which is defined in terms of $f(t)$ as

$$\Phi(\tau) = \frac{1}{1 - \int_0^\tau f(t)dt}. \tag{6}$$

This is the inverse of the probability of observing a waiting time larger than τ or, equivalently, the proportion of transcriptional event intervals that are longer than τ. If the dynamics are bursty, we expect two well-separated timescales for the decay of $f(t)$; correspondingly, Φ will display a plateau and two inflection points. These points, τ_1 and $\tau_2 > \tau_1$, can be found as the zeros in the second derivative of Φ; these values also approximate the two timescales for $f(t)$ (this is not a strict equality but rather an order-of-magnitude estimate). The value of Φ in the middle of the plateau, ($\Phi(\tau_x) = (\Phi(\tau_1) + \Phi(\tau_2))/2$), then yields the average number of transcriptional events in a burst or burst size, β (33). If the dynamics are not bursty, Φ will have no more than one inflection point. An analysis of $f(t)$ and $\Phi(t)$ shows that these criteria work qualitatively well for our model. For sufficiently large values of k_{topo}, we find that the dynamics are indeed bursty (Fig. 1): $f(t)$ has two characteristic timescales (Fig. 1 *b*), and $\Phi(\tau)$ has two well-defined inflection points (Fig. 1 *c*). For small k_{topo} and high values of the flux, there are no well-defined timescales in $f(t)$ or inflection points in $\Phi(\tau)$; inspection of the transcriptional dynamics show this is not bursty (see Fig. S3 *c*).

To quantify the burstiness of a transcriptional time series, we define the following parameter,

$$\xi = \frac{\Phi'(\tau_1) - \Phi'(\tau_2)}{\Phi'(\tau_1)}, \tag{7}$$

which measures the area under $\Phi''(\tau)$ between the two inflection points (when they exist), normalized by $\Phi'(\tau_1)$ so that the result remains between 0 and 1 (prime and double prime denote the first and second derivatives, respectively). ξ is zero when the dynamics are not bursty and increases as the separation between the two characteristic timescales τ_1 and τ_2 becomes clearer: we refer to this parameter as the burst significance.

RESULTS AND DISCUSSION

A single gene

We first consider the case of a single gene. By computing ξ from simulations with different values of $\overline{J}/D$ and k_{topo}/k_0, we find two distinct regimes (Fig. 2 *a*): the nonbursty regime, identified by $\xi = 0$, and the bursty regime, for $\xi > 0$ (a mean field theory gives a good prediction of the boundary between the two). In the most significant region ($k_{\text{topo}}/k_0 \sim 1.4$, $\overline{J}/D \sim 1.5$), the burst size is between 2 and 3, close to that measured in *E. coli* in vivo (6). Estimates of the other bursts parameters (i.e., burst duration and OFF-state duration) are given in Supporting Materials and Methods (Section SIII) and are also in good agreement with experimental results (6,14). However, we note that the burst size depends on the model parameters: the system can produce bursts of significantly more than two to three events (at most ~10 on average in our simulations). However, this only occurs in the transition region between the nonbursty and bursty regimes (see Fig. S2 *a*). In this transition region, burst significance is smaller, which means that the separation between timescales is less marked.

The results in Fig. 2 *a* also show that when the positive feedback between supercoil generation and transcription initiation is strong (for large $\overline{J}/D$ and $k_{\text{topo}} = 0$, identified as the supercoiling-regulated regime of (16)), the dynamics are never bursty; bursts are most significant when this feedback is much weaker (but nonzero). The reason for this seemingly surprising result is that if supercoiling upregulates transcription too much, the gene is essentially always on and the transcriptionally silent state is absent (see Fig. S3 *c*).

Our results show that topoisomerase action favors burstiness. In other words, although the dynamics can be bursty for $k_{\text{topo}} = 0$, burst significance is larger when $k_{\text{topo}} \neq 0$.

Since bursting is generally due to switching back and forth between two transiently stable states, it is natural to ask whether there are any signatures of bistability in the stochastic transcriptional process we simulate. As we show in Fig. 2 *b*, one such signature can be obtained from moments of the distribution of supercoiling at the promoter σ_p. For nonbursty behavior, σ_p exhibits close-to-Gaussian fluctuations about an average value (see Fig. S3 *b*). For bursty transcription, this distribution is more markedly non-Gaussian

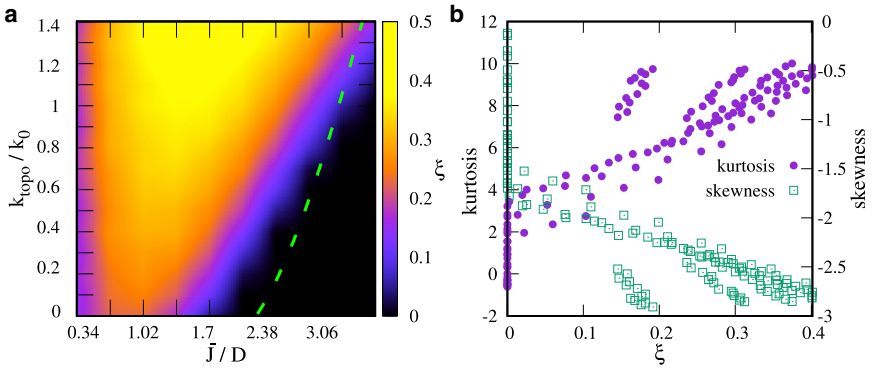

FIGURE 2 Burstiness for a single gene. (*a*) A phase diagram shows the burst significance as a function of model parameters. A nonbursty regime is indicated by $\xi = 0$ (*black*), whereas $\xi > 0$ indicates a bursty regime (*yellow-red*). The dashed green line is the boundary predicted via mean field (see Supporting Materials and Methods, Section SI). (*b*) Non-Gaussian parameters of the distribution of the supercoiling at the promoter σ_p as a function of ξ, for different values of $\overline{J}/D$ and k_{topo}/k_0 are shown. The kurtosis (skewness) is correlated (anticorrelated) with ξ. To see this figure in color, go online.

and bistable (see Fig. S3 *a*). Quantitatively, burst significance correlates with the magnitude of non-Gaussianity parameters such as kurtosis and skewness (Fig. 2 *b*; Fig. S3).

Multiple genes

The single-gene case considered above is an important starting point for our model and could be relevant to the experimental investigation in (6), where the transcription of a gene on a bacterial plasmid was monitored. However, it is also of interest to consider the case of multiple genes. This is because gene density is variable both across organisms and within genomes: for instance, in both yeast and bacteria, gene density is high so that transcription is likely to affect neighboring genes. This is also relevant for understanding synthetic DNA constructs containing multiple genes, which can be used in biotechnology applications. In this section, we study the burstiness in arrays of multiple genes without topoisomerases (i.e., $k_{topo} = 0$).

In Fig. 3, we consider the supercoiling-coupled transcriptional dynamics within an array of genes, which have the same orientation (we refer to these as "tandem" genes). We find that bursts are typically more significant than in the single-gene case. For instance, for $\overline{J}/D = 1$ and $k_{topo} = 0$, the single-gene case was only weakly bursty ($\xi \approx 0.23$, burst size $\beta \approx 1.53$, and duration $T \approx 100$ s (see Fig. S2)), whereas for an array of 10 tandem genes, the same parameters give rise to bursting, which is approximately twice as significant ($\xi \approx 0.4$–0.5 for the most bursty genes, burst size $\beta \approx 2$, and duration $T \approx 3$–4 min (see Fig. S7)). This is because transcription generates positive supercoils ahead of a gene, which act to downregulate its downstream (right) neighbor (while upregulating the upstream [left] neighbor). As a result, some genes may be transiently "switched off"; this can be

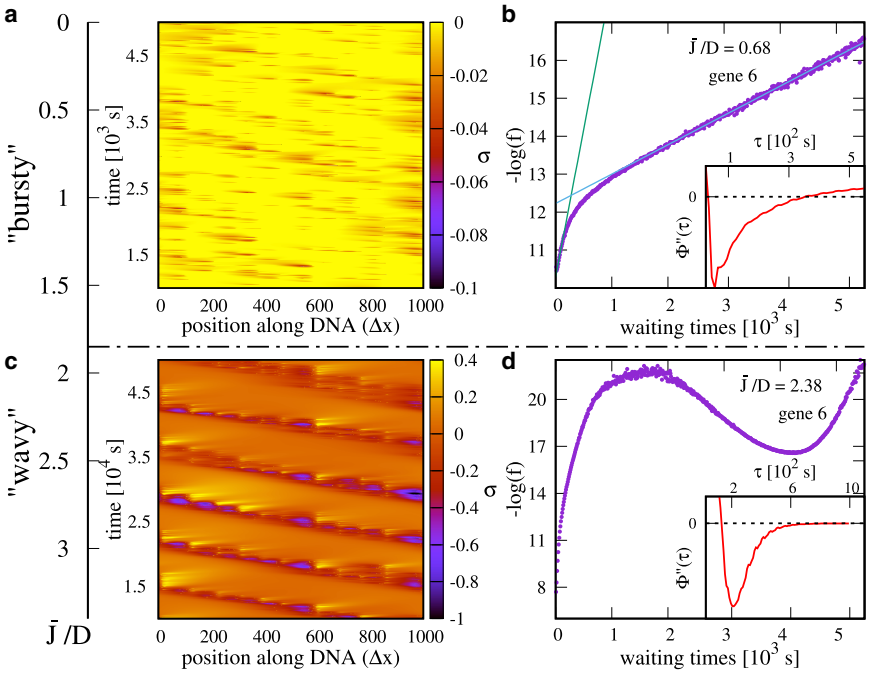

FIGURE 3 Bursty and wavy regimes for an array of 10 tandem genes. (*a*) A kymograph in the bursty regime ($\overline{J}/D = 0.68$) is shown. For clarity, we only show the negative supercoiling range. There are correlations between neighboring genes but no clear periodic pattern. Note that genes 1 and 10 turn red more often (compare to genomic map in Fig. 5 *a*) because they are slightly upregulated. (*b*) A plot of the pdf of waiting times in the bursty regime, showing the emergence of two timescales is shown. The inset shows the second derivative of the ssf, which displays two zeros. (*c*) A kymograph in the supercoiling-regulated regime ($\overline{J}/D = 2.38$) is shown. For high values of the flux, the bursty dynamics are replaced by transcription waves. (*d*) The pdf of waiting times in the supercoiling-regulated regime is shown. The new timescale associated with the wave modifies the shape of the distribution, giving rise to a "bump" at $\sim 4 \times 10^3$ s (local minimum in linear-log plot). The inset shows the second derivative of ssf. In the physically relevant range of waiting times ($\tau \lesssim 10^3$ s), the function asymptomatically approaches zero without crossing the axis ($\tau_2 \to +\infty$).To see this figure in color, go online.

appreciated, for instance, by inspecting the time series of supercoiling at the promoter, which at times can take sufficiently positive values such that $k_{in}(t) = 0$, see Fig. S5 *a*. Just as in the case of a single gene with $k_{topo} \neq 0$, the activity of each gene is effectively described by a two-state dynamics (ON $\leftrightarrow$ OFF), and bursts can occur (Fig. 3 *a*). As expected, the pdf of waiting times is well described by a double exponential (see Fig. 3 *b*) and $\Phi''(\tau)$ displays two zeros (Fig. 3 *b*, *inset*).

As for the single-gene case, in the multigene system, bursting does not occur for large values of $\overline{J}/D$. In this regime, the supercoiling-mediated intergenic interactions instead give rise to transcription waves, which travel in the opposite direction to transcription (Fig. 3, *c* and *d*). Transcription waves arise because transcription of a gene upregulates its upstream (left) neighbor (16): as a consequence, transcription of gene i is followed by that of gene $i-1$, then $i-2$, and so on. We find that the wave velocity is $v \sim D/l$, independent of k_0 (Fig. 4, *inset*; $l = 100\Delta x$ is the mean separation between promoters in our simulations). Given our parameter choice, the wave speed is between 0.5 and 3.0 bp/s, and the time needed to trigger activity of the neighboring upstream gene is between 6 and 12 min. The scaling of v can be understood by assuming that supercoiling propagates diffusively over the distance l between a gene, and its upstream-neighbor; simulation show that the prefactor in this relationship is slightly larger than one. When in the "wavy" regime, the system can no longer be mapped onto a telegraph-like process, and bursts are no longer observed (accordingly, $\xi = 0$ because $\Phi(t)$ does not have two inflection points; see Fig. 3 *d*).

Transcription waves only arise for arrays of tandem genes and do not occur (or do so only transiently) for genes of differing orientation. In that case, transcription-generated supercoiling upregulates pairs of divergent genes at the expense of other (convergent or tandem) genes, which are downregulated (16): this renders the situation qualitatively closer to that of a single gene (see Supporting Materials and Methods, Section SIV). For either kind of gene orientation, burstiness is gene dependent, and the values of ξ for different genes are substantially different from each other (Fig. 5). Note that even for small $\overline{J}/D$, some genes are slightly upregulated than others (as shown in the kymograph in Fig. 3 *a*) because of the particular position in the array. We find that ξ is anticorrelated with the overall transcription rate so that the genes that are expressed more (e.g., genes 1, 6, and 10 in the tandem setup or genes 5 and 6 in the divergent setup; see Figs. 5 *a*, S6, and S9 *a*) are less bursty (Fig. 6 *a*). Burst size is also different in the tandem and bidirectional setups, being substantially smaller in the latter case ($\beta \lesssim 2$; see Fig. S7 *a*). Burst sizes measured experimentally in *E. Coli* (6) are closer to the value for single or tandem genes ($\beta \simeq 2.2$); this is reasonable because they refer to the transcription of operons, which are normally made up from tandem genes controlled by a single promoter.

An analysis of the distribution of supercoiling values at the promoter shows that these differ qualitatively for the cases of multiple genes and a single gene (e.g., compare Fig. 6 with Fig. S3). Unlike in the single-gene case, the non-Gaussian parameters for the distribution of supercoiling at the promoter now only weakly correlate with the burst significance (see Fig. S8). This is because the supercoiling-mediated interaction between genes give rise to non-Gaussian fluctuations even for nonbursty genes. Nevertheless, for both the tandem and divergent gene cases, bursting leaves a detectable signature in the tails of the distribution.

For the bursty transcription case, there is a singularity or a bump, whereas for nonbursty transcription, the curve is smooth, as shown in Fig. 6 *b* for a divergent geometry and in Fig. 6 *c* for a tandem array. The singular point is located at $\sigma_p \approx (1 - (k_0\tau_x)^{-1})/\alpha$, where $\tau_x = (\tau_1 + \tau_2)/2$. We note that similar changes in the behavior of large fluctuations were linked to phase transitions in other systems (35,36).

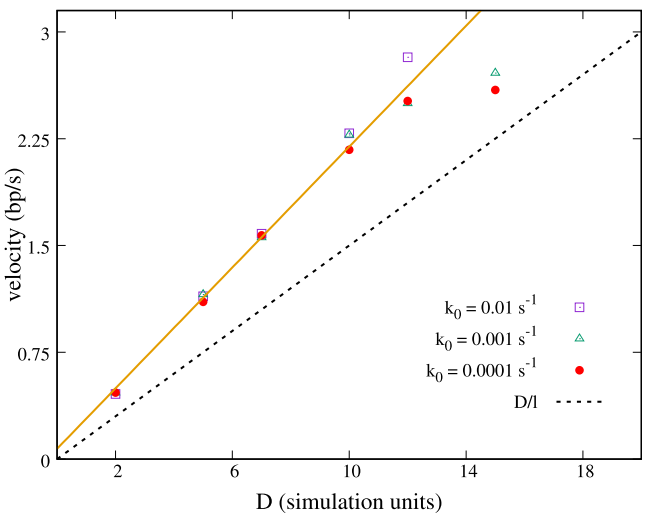

FIGURE 4 Wave velocity and scaling relation. Wave velocity for different values of D ($\overline{J} = 25.5$) and k_0 so that we span a large range of $\overline{J}/D$ values between 1.7 and 12.7. Values of D are given in simulation units (i.e., in units of $\Delta x^2/\Delta t$). Simulation data are well fitted by a straight line (*orange*), whereas the simple scaling theory discussed in the text underestimates the data slightly (*dashed black line*). To see this figure in color, go online.

CONCLUSIONS

In summary, we have studied the occurrence of transcriptional bursts in a nonequilibrium model for supercoiling-regulated transcription, first introduced in (16). For an isolated gene, we found that significant bursting occurs primarily in the presence of topological enzymes, which relax positive and negative supercoiling. This is qualitatively consistent with experimental evidence that bursts in *E. coli* arise because of the action of the DNA gyrase enzyme, which can relax positive supercoiling (14). It is interesting to note that in the region of parameter space where bursts are most significant, the properties of the bursts generated in the model (size, duration, and interburst time)

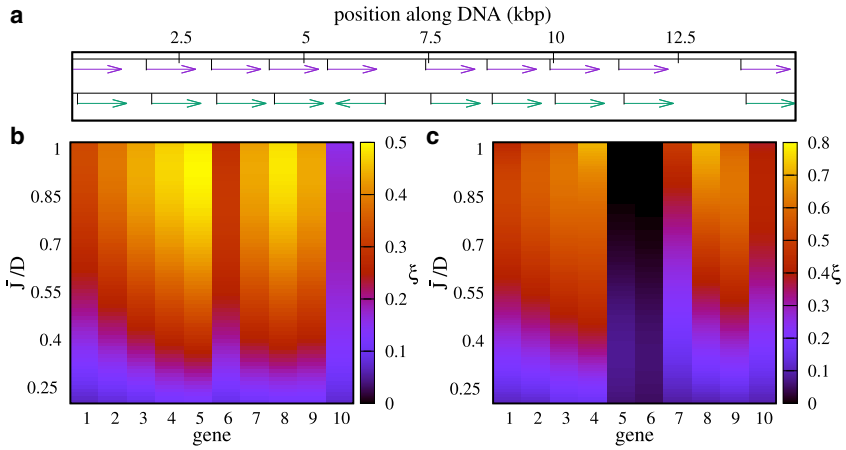

FIGURE 5 Burstiness for a multiple-gene array. (*a*) A map of gene positions for tandem (*top*) and divergent geometry (*bottom*) is shown. (*b* and *c*) A plot of ξ for tandem geometry (*b*) and divergent geometry (*c*) (geometries used are in *a*) is shown. The range of $\overline{J}/D$ (0.06–1.02) is chosen so that the system is in the bursty regime. To see this figure in color, go online.

match well with those found in bacteria in vivo (6). Notably, topoisomerase action is not required for highly significant bursting in gene clusters because there, supercoiling can mediate transient inhibition of the neighbors of highly active genes. We considered both tandem and bidirectional gene geometries, which could be recreated synthetically using plasmids of selected sequence in the presence of the transcriptional machinery. We found that the existence of bursting is intimately linked to the nature of fluctuations of supercoiling at gene promoters: bursting becomes most significant when these are strongly non-Gaussian. It would be of interest to look for such effects in experiments with populations of synthetic DNA loops for which psoralen binding (17,18) might, in principle, be used to monitor averages and distributions of supercoiling along the DNA.

Although additional ingredients may be required to understand transcriptional bursts in eukaryotes, in which stochastic promoter-enhancer interactions or other regulatory processes are known to play a key role (2,13,37), our current results uncover a possible mechanism for transcriptional bursts in bacteria based on the interplay between transcription initiation, supercoiling, and topological enzymes. Our results are consistent with the work in (9), which identified supercoiling as one potential mechanism for bursting based on the comparison between experimental data and a simplified kinetic model; in our case, we consider a full stochastic dynamics for supercoiling

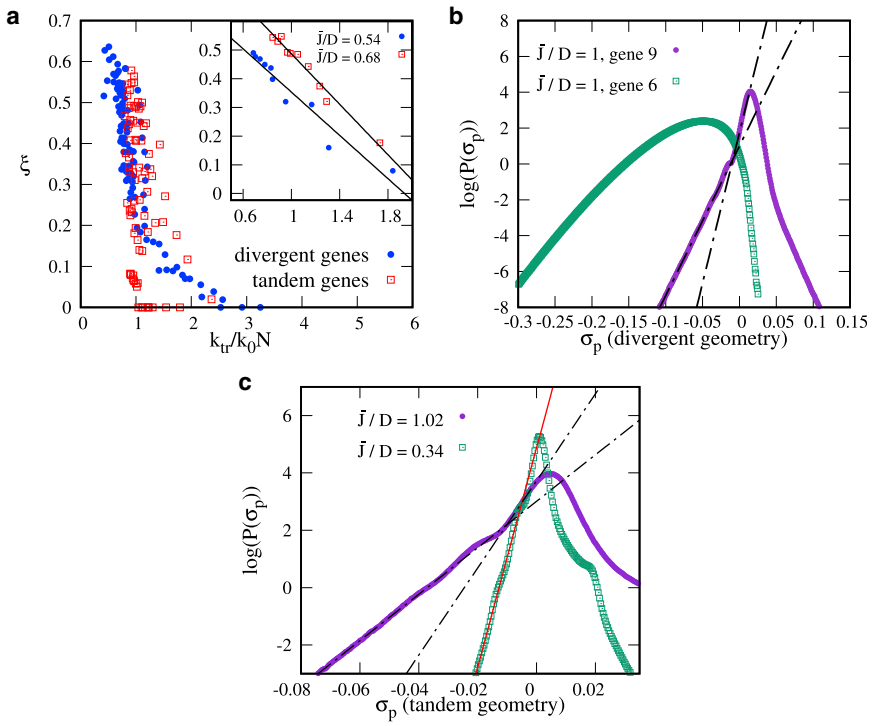

FIGURE 6 Bursty and wavy regimes for an array of 10 tandem genes. (*a*) The burstiness, ξ, is plotted for a different value of the overall time-averaged transcription rate k_{tr} for tandem (*red squares*) and bidirectional (*blue circles*) genes (each point represents a gene; points are shown for different values of $\overline{J}/D$ between 0.06 and 1.02). The inset shows that for a given value of $\overline{J}/D$, ξ depends linearly on k_{tr} (each point represents a gene). (*b*) A log-linear plot of the distribution of σ_p is shown. For bursty genes (gene 9, which is not part of the divergent pair), this distribution shows a singularity or bump. Such a singularity does not appear for highly transcribed genes (gene 6, in the divergent pair). (c) For a given gene (gene 4, tandem geometry), the slope of the negative tail of the distribution depends on $\overline{J}/D$. For small ξ (small $\overline{J}/D$), the bump disappears. To see this figure in color, go online.

and elucidate the role of topoisomerases. As discussed in the Introduction, a related study (12) instead analyzed the interplay between supercoiling and transcriptional elongation, providing a complementary mechanism to the one identified here; that model may be particularly relevant for the case of ribosomal genes for which expression is extremely high, whereas our work concerns more moderate expression for which there is not significantly more than one polymerase transcribing the same gene at once.

SUPPORTING MATERIAL

Supporting Material can be found online at https://doi.org/10.1016/j.bpj.2019.04.023.

AUTHOR CONTRIBUTIONS

M.A., A.B., C.A.B., G.G., and D.M. designed research. M.A. and A.B. performed simulations. M.A. analyzed data. M.A., A.B., C.A.B., G.G., and D.M. wrote the article.

ACKNOWLEDGMENTS

Simulations were run at Bari ReCas e-Infrastructure funded by Ministero dell'Istruzione, through the National Operational Programme Research and Competitiveness 2007–2013 Call 254 Action I. We acknowledge support from European Research Council (CoG 648050, THREEDCELLPHYSICS).

REFERENCES

1. Alberts, B., D. Bray, …, M. Raff. 2002. Molecular Biology of the Cell. Garland Science, New York.
2. Raj, A., and A. van Oudenaarden. 2008. Nature, nurture, or chance: stochastic gene expression and its consequences. *Cell.* 135:216–226.
3. Berg, O. G., R. B. Winter, and P. H. von Hippel. 1981. Diffusion-driven mechanisms of protein translocation on nucleic acids. 1. Models and theory. *Biochemistry.* 20:6929–6948.
4. Halford, S. E., and J. F. Marko. 2004. How do site-specific DNA-binding proteins find their targets? *Nucleic Acids Res.* 32:3040–3052.
5. Schwanhäusser, B., D. Busse, …, M. Selbach. 2011. Global quantification of mammalian gene expression control. *Nature.* 473:337–342.
6. Golding, I., J. Paulsson, …, E. C. Cox. 2005. Real-time kinetics of gene activity in individual bacteria. *Cell.* 123:1025–1036.
7. Losick, R., and C. Desplan. 2008. Stochasticity and cell fate. *Science.* 320:65–68.
8. Gardiner, C. W. 2004. Handbook of Stochastic Methods: For Physics, Chemistry, and the Natural Science. Springer, New York.
9. Mitarai, N., I. B. Dodd, …, K. Sneppen. 2008. The generation of promoter-mediated transcriptional noise in bacteria. *PLoS Comput. Biol.* 4:e1000109.
10. Suter, D. M., N. Molina, …, F. Naef. 2011. Mammalian genes are transcribed with widely different bursting kinetics. *Science.* 332:472–474.
11. Harper, C. V., B. Finkenstä, …, D. Woodcock. 2011. Long-term unsynchronised transcriptional cycles individual living mammalian cells. *PLoS Biol.* 9:1000607.
12. Sevier, S. A., and H. Levine. 2018. Properties of gene expression and chromatin structure with mechanically regulated elongation. *Nucleic Acids Res.* 46:5924–5934.
13. Corrigan, A. M., E. Tunnacliffe, …, J. R. Chubb. 2016. A continuum model of transcriptional bursting. *eLife.* 5:e13051.
14. Chong, S., C. Chen, …, X. S. Xie. 2014. Mechanism of transcriptional bursting in bacteria. *Cell.* 158:314–326.
15. Bates, A. D., and A. Maxwell. 2005. DNA Topology. Oxford University Press, New York.
16. Brackley, C. A., J. Johnson, …, D. Marenduzzo. 2016. Stochastic model of supercoiling-dependent transcription. *Phys. Rev. Lett.* 117:018101.
17. Naughton, C., N. Avlonitis, …, N. Gilbert. 2013. Transcription forms and remodels supercoiling domains unfolding large-scale chromatin structures. *Nat. Struct. Mol. Biol.* 20:387–395.
18. Kouzine, F., A. Gupta, …, D. Levens. 2013. Transcription-dependent dynamic supercoiling is a short-range genomic force. *Nat. Struct. Mol. Biol.* 20:396–403.
19. Kamien, R. D. 1998. Local writhing dynamics. *Eur. Phys. J. B.* 1:1–4.
20. Chaikin, P. M., and T. C. Lubensky. 1995. Principles of Condensed Matter Physics. Cambridge University Press, Cambridge, UK.
21. van Loenhout, M. T., M. V. de Grunt, and C. Dekker. 2012. Dynamics of DNA supercoils. *Science.* 338:94–97.
22. Moulin, L., A. R. Rahmouni, and F. Boccard. 2005. Topological insulators inhibit diffusion of transcription-induced positive supercoils in the chromosome of *Escherichia coli*. *Mol. Microbiol.* 55:601–610.
23. Liu, L. F., and J. C. Wang. 1987. Supercoiling of the DNA template during transcription. *Proc. Natl. Acad. Sci. USA.* 84:7024–7027.
24. Marko, J. F. 2007. Torque and dynamics of linking number relaxation in stretched supercoiled DNA. *Phys. Rev. E Stat. Nonlin. Soft Matter Phys.* 76:021926.
25. Liang, S., M. Bipatnath, …, H. Bremer. 1999. Activities of constitutive promoters in *Escherichia coli*. *J. Mol. Biol.* 292:19–37.
26. Pelechano, V., S. Chávez, and J. E. Pérez-Ortín. 2010. A complete set of nascent transcription rates for yeast genes. *PLoS One.* 5:e15442.
27. Jackson, D. A., A. Pombo, and F. Iborra. 2000. The balance sheet for transcription: an analysis of nuclear RNA metabolism in mammalian cells. *FASEB J.* 14:242–254.
28. Bremer, H. D., and P. P. Dennis. 1996. *In* Escherichia Coli and Salmonella: Cellular and Molecular Biology, Second Edition, F. C. Neidhardt, ed. ASM Press, p. 1553.
29. Ishihama, Y., T. Schmidt, …, D. Frishman. 2008. Protein abundance profiling of the *Escherichia coli* cytosol. *BMC Genomics.* 9:102.
30. Terekhova, K., K. H. Gunn, …, A. Mondragón. 2012. Bacterial topoisomerase I and topoisomerase III relax supercoiled DNA via distinct pathways. *Nucleic Acids Res.* 40:10432–10440.
31. Weintraub, H., P. F. Cheng, and K. Conrad. 1986. Expression of transfected DNA depends on DNA topology. *Cell.* 46:115–122.
32. Rhee, K. Y., M. Opel, …, G. W. Hatfield. 1999. Transcriptional coupling between the divergent promoters of a prototypic LysR-type regulatory system, the ilvYC operon of *Escherichia coli*. *Proc. Natl. Acad. Sci. USA.* 96:14294–14299.
33. Dobrzyński, M., and F. J. Bruggerman. 2009. Elongation dynamics shape bursty transcription and translation. *Proc. Natl. Acad. Sci. USA.* 106:2583–2588.
34. Kumar, N., A. Singh, and R. V. Kulkami. 2015. Transcriptional bursting in gene expression: analytical results for general Stochastic models. *PLoS Comput. Biol.* 11:e1004292.
35. Cagnetta, F., F. Corberi, …, A. Suma. 2017. Large fluctuations and dynamic phase transition in a system of self-propelled particles. *Phys. Rev. Lett.* 119:158002.
36. Janas, M., A. Kamenev, and B. Meerson. 2016. Dynamical phase transition in large-deviation statistics of the Kardar-Parisi-Zhang equation. *Phys. Rev. E.* 94:032133.
37. Fukaya, T., B. Lim, and M. Levine. 2016. Enhancer control of transcriptional bursting. *Cell.* 166:358–368.

Biophysical Journal, Volume *117*

Supplemental Information

Transcriptional Bursts in a Nonequilibrium Model for Gene Regulation by Supercoiling

Marco Ancona, Alessandro Bentivoglio, Chris A. Brackley, Giuseppe Gonnella, and Davide Marenduzzo

I. MEAN FIELD THEORY

Here, we develop a mean field theory with some improvements with respect to our previous work [1]. In particular we solve the mean field ordinary differential equation (ODE) with periodic boundary conditions (instead of open boundary conditions, as previously done) and in the presence of topoisomerases.

We consider the case $N = n = 1$, where N is the number of RNAP and n is the number of genes. Besides, we consider a *static* polymerase (i.e. $v = 0$) at the lattice position $x = 0$. If L is the length of the lattice, we assume boundary conditions $\sigma(0) = 0$ and $\sigma(L/2) = \sigma(-L/2)$. In steady state ($\partial\sigma/\partial t = 0$), Eq. (1) reads:

$$\frac{\partial^2\sigma(x)}{\partial x^2} - \frac{J_0}{D}\frac{k_{\rm in}\tau}{k_{\rm in}\tau+1}\frac{\partial\delta(x)}{\partial x} - \frac{k_{\rm topo}}{D}\sigma(x) = 0 \tag{S1}$$

where we have made the mean field approximation

$$\frac{J_{tr}(x,t)}{D} \to \frac{J_0}{D}\frac{k_{\rm in}\tau}{k_{\rm in}\tau+1}\delta(x) \equiv M\delta(x) \tag{S2}$$

with $k_{\rm in}\tau/(k_{\rm in}\tau+1)$ the fraction of time the system spends in the transcribing state.

As the flux term acts only at $x = 0$, solving the model in the mean field approximation is equivalent to solving the following ODE:

$$\begin{cases} \dfrac{\partial^2\sigma(x)}{\partial x^2} - \dfrac{k_{\rm topo}}{D}\sigma(x) = 0 & x \neq 0 \\[2ex] \left.\dfrac{\partial\sigma(x)}{\partial x}\right|_{x=0} = M\delta(0) \\[2ex] \sigma\left(L/2\right) = \sigma\left(-L/2\right). \end{cases} \tag{S3}$$

Since both $\sigma(x)$ and $\sigma(-x)$ are solution of the ODE for $x \neq 0$ the unique solution of Eq. (S3) is a linear combination of $\sigma(x)$ and $\sigma(-x)$. It can be shown that only the antisymmetric combination fulfils the periodic boundary conditions, with $\sigma(L/2) = \sigma(-L/2) = 0$.

The solution of Eq. (S3) with the appropriate parity and boundary conditions is given

by:

$$\sigma(x) = \frac{M}{2} \frac{\sinh\left[\sqrt{\frac{k_{\text{topo}}}{D}}\left(\frac{L}{2} - |x|\right)\right]}{\sinh\left[\sqrt{\frac{k_{\text{topo}}}{D}}\frac{L}{2}\right]} \text{sgn}(x), \tag{S4}$$

where sgn(x) is the *sign function*. From Eq. (S4) it can be easily shown that in the limit $k_{\text{topo}} \to 0$ we obtain:

$$\sigma(x) = \frac{M}{2}\left(1 - \frac{2|x|}{L}\right)\text{sgn}(x). \tag{S5}$$

The term proportional to $1/L$ is the correction due to the periodic boundary conditions, that disappears for $L \to \infty$, recovering the solution in Ref. [1]. In the limit $L \to \infty$, with finite k_{topo}, we have

$$\sigma(x) = \frac{M}{2}\exp\left(-\sqrt{\frac{k_{\text{topo}}}{D}}|x|\right)\text{sgn}(x). \tag{S6}$$

The validity of this mean field theory can be determined by comparing it to the time-average supercoiling profile in our single gene simulations.

Interestingly, from our simulations we found that the point along the gene at which the time-averaged supercoiling profile crosses zero is $\sim 2\lambda/3$, independently of the parameter used. The correct mean field profile of supercoiling for a moving polymerase is then computed by substituting $|x| \to |x - 2\lambda/3|$.

II. THE MODIFIED *IPP* PROCESS

The mechanism which leads to bursty dynamics for transcription in living cells is still not well understood, though several hypothesis have been made. In our model, we have seen that both the action of topoisomerases (1-gene model) and the interaction among genes (10-gene model) can yield bursts, in absence of external factors. The nontrivial nonlinear behaviour predicted by our model can be captured by a simpler kinetic scheme: the *Interrupted Poisson Process* (*IPP*). By solving the *IPP* equations, one can explicitly obtain the double-exponential distribution of waiting times between events, that, when appropriate conditions on the kinetics rates are met, leads to bursting. In this section we modify the *IPP* equations. Nevertheless, the resulting distribution is still a double-exponential (see below), with the exception of the two timescales, which are different from those found in [2].

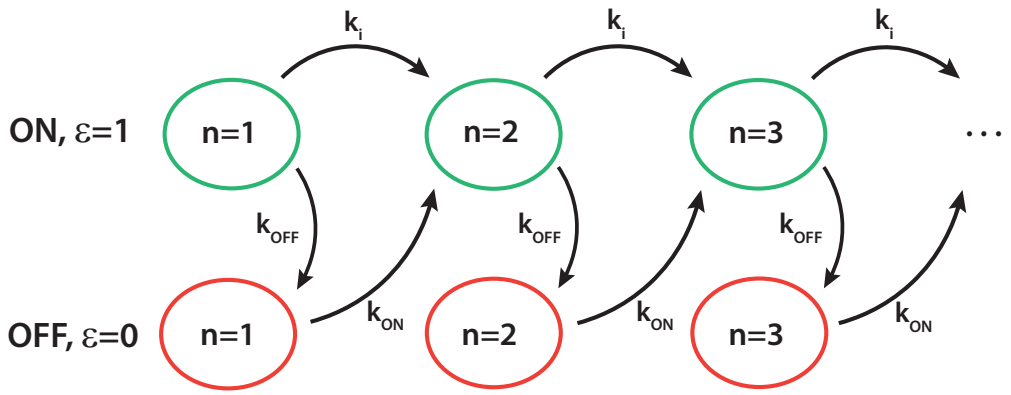

FIG. S1: **Scheme of the discrete states in a *modified IPP*.** Each *box* represent a state, with $\epsilon \in \{0, 1\}$. The index n labels the number of initiation events.

We define (as in Fig. 1a of the main text) an *active* (ON, or $\epsilon = 1$) and an *inactive* (OFF, or $\epsilon = 0$) state of the gene promoter according to the local supercoiling density (i.e., if the supercoiling density is below $(1 - (k_0\tau_2)^{-1})/\alpha$, then the promoter is ON). We then associate the rates k_{OFF} and k_{ON} with the $ON \to OFF$ and $OFF \to ON$ transitions respectively. The gene oscillates between the two states, tracking the typical trajectories of a *Random Telegraph Process* (see Fig. 1a, BOTTOM). Whilst in the ON state, the gene is able to transcribe with rate k_i. Given a time series of events, the *waiting time* t_n is the elapsed time between two consecutive transcriptions, say the $(n-1)$-th and the n-th. In the *IPP*, the waiting time t_n is drawn by the same probability distribution function (*pdf*) for each n (this may not be true in general in our stochastic model for supercoiling-dependent transcription). Moreover, in the standard *IPP* prescription the $OFF \to ON$ transition occurs between states labelled by the same n, see Ref. [2]. Differently, in our modified *IPP* description, the transition $OFF \to ON$ is triggered by transcription (see Fig. S1), meaning that the transition and the first event in the burst occur at the same time. By labelling possible states with the instantaneous value of ϵ (gene ON/OFF) and by the index n, which keeps count of the number of transcriptions, we denote the probability of being in the state $\{n, \epsilon\}$ at time t by $p_{n,\epsilon}(t)$. Then, the set of master equations for our modified *IPP* is:

$$\begin{cases} \dfrac{dp_{1,1}(t)}{dt} = -(k_i + k_{OFF})\ p_{1,1}(t) \\ \dfrac{dp_{n,1}(t)}{dt} = k_i p_{n-1,1}(t) + k_{ON} p_{n-1,0}(t) - (k_i + k_{OFF}) p_{n,1}(t), \qquad n = 2, 3, \dots \\ \dfrac{dp_{n,0}(t)}{dt} = k_{OFF}\ p_{n,1}(t) - k_{ON}\ p_{n,0}(t) \qquad n = 1, 2, \dots \end{cases} \tag{S7}$$

with the initial condition $p_{1,1}(t = 0) = 1$. Clearly, the *pdf* associated with the first transcription event after initialisation ($n = 2$) corresponds to the distribution of waiting times, that is

$$f(t) = k_i\ p_{1,1}(t) + k_{ON}\ p_{1,0}(t). \tag{S8}$$

In order to find $p_{1,1}(t)$ and $p_{1,0}(t)$, and therefore $f(t)$, we need to solve just the following two first order coupled ODEs:

$$\begin{cases} \dfrac{dp_{1,1}(t)}{dt} = -(k_i + k_{OFF})\ p_{1,1}(t), \\ \dfrac{dp_{1,0}(t)}{dt} = k_{OFF}\ p_{1,1}(t) - k_{ON}\ p_{1,0}(t). \end{cases} \tag{S9}$$

By solving Eq. (S9) and using Eq. (S8), we have

$$f(t) = w_1 r_1 e^{-r_1 t} + w_2 r_2 e^{-r_2 t}, \tag{S10}$$

with rates $r_{1,2}$

$$r_1 = k_i + k_{OFF}, \qquad r_2 = k_{ON}, \tag{S11}$$

and weights $w_{1,2}$

$$w_1 = \frac{k_i - r_2}{r_1 - r_2}, \qquad w_1 \in [0, 1]\,, \tag{S12}$$

$$w_2 = 1 - w_1. \tag{S13}$$

In our stochastic model used in the main text, we can identify $k_{ON} \sim k_0$. Conversely, it is not easy to find a value for the rate k_{OFF} without fitting the data, since the transition $ON \rightarrow OFF$ is mainly due to fluctuations, that, in the bursty phase, relax the system towards the initial value of the supercoiling σ_0.

III. 1-GENE ARRAY: BURST PARAMETERS AND ADDITIONAL FIGURES

In our work we use the *sequence-size function*, $\Phi(\tau)$, to analyse burst significance. Although this method has been presented in previous works [2, 3], it has not previously been

applied to simulation of the dynamics of transcription which does not use predetermined kinetic rates for the process.

We use the parameter ξ as defined in Eq. (7) in the main tex, which is different from the parameter proposed in [2], $(\tau_2 - \tau_1)/\tau_2$. Indeed, the former parameter does show variation within the bursty phase, whereas the latter does not. Our parameter ξ yields a reasonable estimate of burst significance, as (i) it is still proportional to $\tau_2 - \tau_1$ and (ii) it fulfils the intuitive expectation that the burst significance should decrease if the system spends more time in intermediate states, at fixed $\tau_2 - \tau_1$.

The analysis of the *ssf* allows us to readily compute other relevant burst parameters in a relatively simple way. The time separation between the two timescales is just $\tau_x = (\tau_1 + \tau_2)/2$ and, from the definition of the *ssf*, we can estimate the *mean burst size* (the average number of transcriptions in a single burst) as $\beta = \Phi(\tau_x)$. This is a useful parameter, since it provides a simple basis to compare with experimental data. As we can see from Fig. S2 higher values of β ($\beta > 4 - 5$) correspond to less significant bursting (see main text, Fig. 2). Conversely, in the region of higher ξ ($\bar{J}/D \sim 1.5 - 2$), the burst size $\beta \simeq 2.2$ is short and close to that experimentally observed in E. Coli [4]. The burst *duration* – i.e. the time duration of a

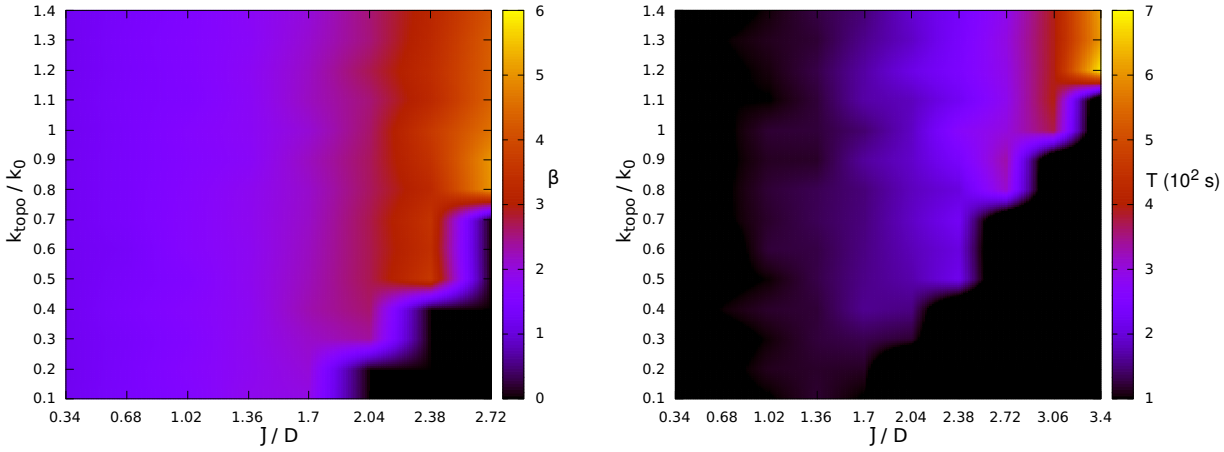

FIG. S2: **Burst size and burst duration for a single gene**. **(a)** Here, we show the burst size β up to $\bar{J}/D = 2.72$, in order to highlight the region of higher burst significance ($\bar{J}/D \sim 1.5 - 2$), in which β is in agreement with experimental measurement of the same parameter [4]. **(b)** Duration of bursts T. We find that in the same region the duration of bursts is also consistent with [4], as $T \sim 3 - 4$ min.

single burst – is estimated by $\beta\tau_x$: in the same parameter region it is also consistent with experimental results [4, 5], $T \sim 3 - 4$ min.

In Fig. S3a,b we present the typical probability distribution of supercoiling at the promoter, respectively in the bursty and non-bursty phases. Within our stochastic model, the supercoiling at the promoter is directly linked to the probability of initiation, and therefore its distribution encodes all of the information about the process. As expected, for bursty dynamics we observe a bimodal distribution of σ_p, while for non-bursty dynamics we have a unimodal distribution, with fluctuations approximately Gaussian.

For completeness, in Fig. S4 we consider a situation where there is a single gene but three polymerases. The rationale is that *in vivo*, at any given time, there can be more than one polymerase available for a given gene, even if the ratio of the total number of RNAP and genes is small. In this multiple polymerase case we find qualitatively similar results to the single polymerase case treated in the text, but only if we increase k_{topo} by a factor of 10. However, the burst significance is remarkably smaller than the case studied in the main text. Nevertheless, the physical features of the bursts are consistent with those of the single polymerase case: e.g., for $\bar{J}/D \sim 1$ we find $\beta \sim 3$ and $T \sim 2$ min.

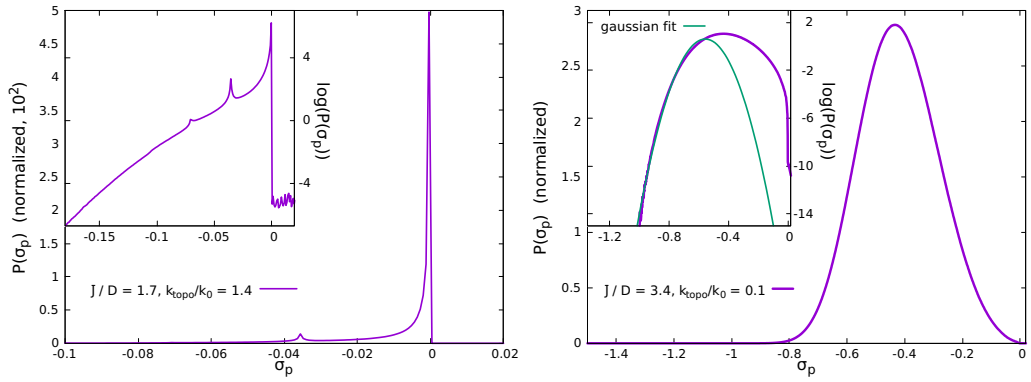

(a) **(b)**

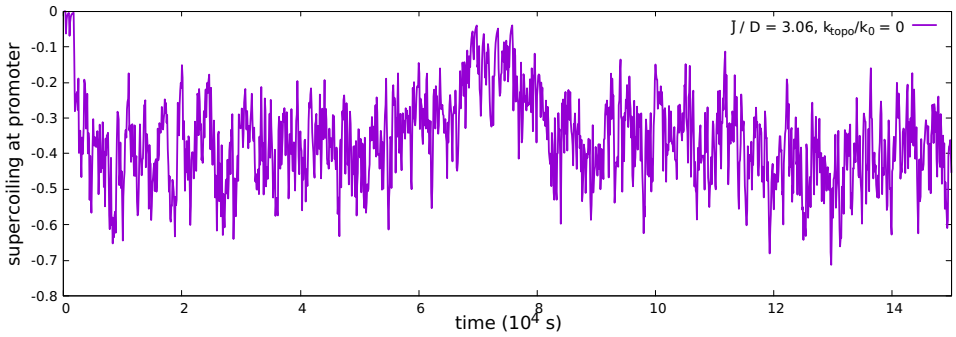

(c)

FIG. S3: **Probability distribution for supercoiling at the promoter**. **(a)** In the bursty phase, supercoiling at the promoter is strongly peaked at $\sigma_p \sim 0$. Another peak appears for more negative value of supercoiling, due to occupation of the ON state. Inset: log-linear plot of the *pdf* in the main panel. **(b)** In the non-bursty phase the distribution is unimodal, with one gaussian tail. The gene tends to more often be in a state with less negative supercoiling for longer time; this results in a non-gaussian positive tail, with a nonzero kurtosis (see main text). **(c)** Time profile of the supercoiling at the promoter in the non-bursty regime. Clearly, the gene is always ON, as the supercoiling does not relax to the initial value $\sigma_0 = 0$.

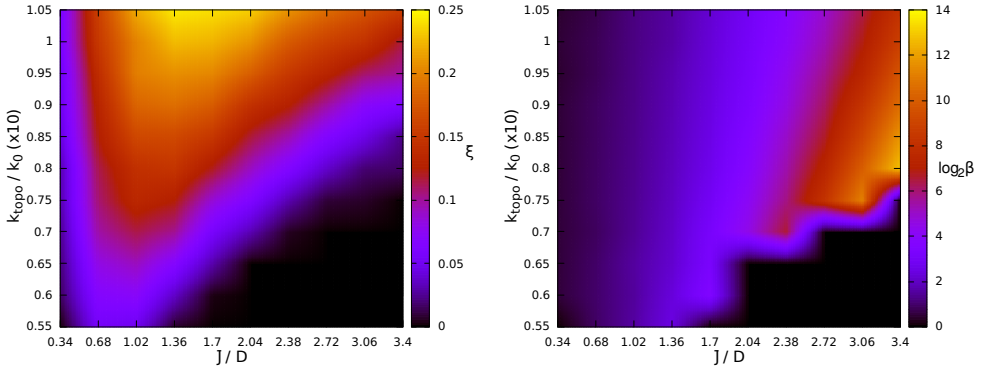

(a) **(b)**

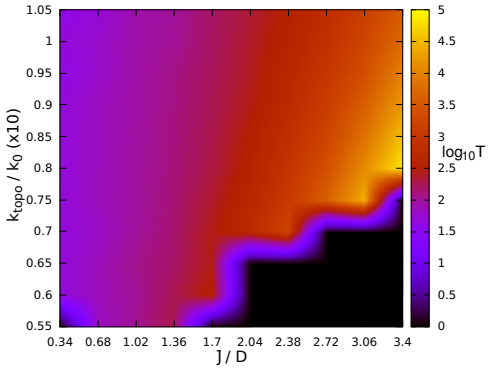

(c)

FIG. S4: **Burst parameters for a single gene and three polymerases**. **(a)** Burst significance ξ. There are still two phases separated by a crossover. **(b,c)** Burst size β and bursts duration T. With respect to the single gene case, here we have a large region of very high values (not biologically relevant) for both the burst size and the duration. However, these correspond to a region of low burst significance; in the region where burst significance is maximal we again find values for β and T consistent with experiments ($\beta \sim 3$, $T \sim 2$ min).

IV. MULTIPLE GENE SIMULATIONS: ADDITIONAL FIGURES

We present some additional results from the 10-gene array simulations for the case $k_{topo} = 0$, for which the main results are presented in the main text.

In the case of tandem genes, for the configuration shown in the main text (see Fig. 5a) the genes 1, 6 and 10 are upregulated by supercoiling. These genes have a larger space upstream of them, so are less affected by the repressive action of positive supercoils generated at their upstream neighbour. This occurs, albeit to a much lesser extent, even in the relaxed regime. This relatively small upregulation is sufficient to yield a sizeable change in the burst significance (see main text, Fig. 5b).

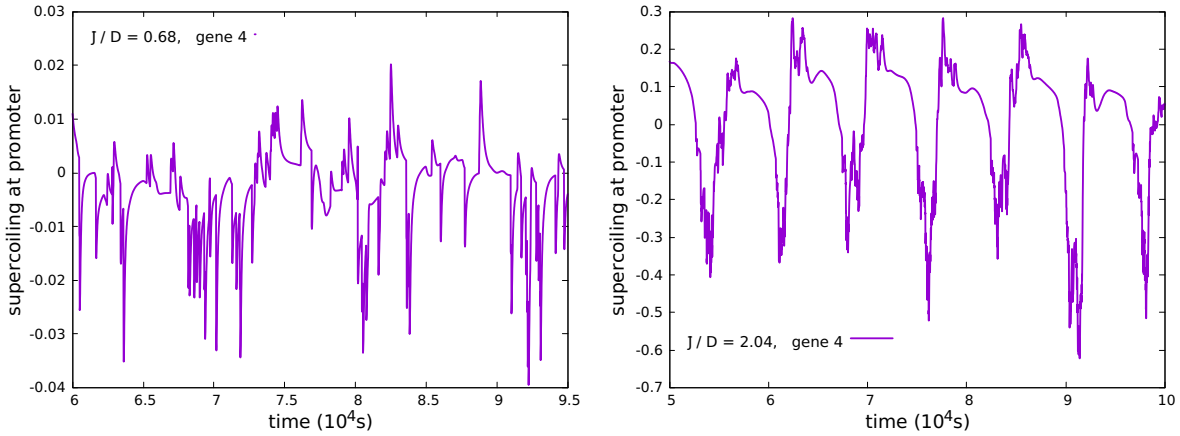

(a) **(b)**

FIG. S5: **Supercoiling dynamics at the promoter gene 4 in a 10-gene array**. **(a)** Promoter supercoiling versus time in the bursty regime. For $\bar{J}/D$ sufficiently small correlation between neighbours genes are established. Positive supercoiling produced by gene 3 transcription often freezes gene 4, yielding the supercoiling value transiently to the absorbing state ($\sigma_0 = 0.01$, $k_{in} = 0$). **(b)** Promoter supercoiling versus time in the supercoiling-regulated regime. In this regime the correlation spreads through the whole lattice, creating a transcription wave. Supercoiling at the promoter now oscillates in time.

In Fig. S5a we show a typical time series for the supercoiling at the promoter of the gene 4 (which is not upregulated), when the burst significance is high ($\bar{J}/D = 0.68$, that is in the bursty transcriptional regime). In Fig. S5b we show the supercoiling time series in the *wavy* regime: a periodic pattern appears so that the dynamics is no longer bursty. In Figure

Fig. S6 we show the probability of transcription for each gene, in the bursty regime, for two different values of the flux $\bar{J}/D$.

In Fig. S7 we show the mean size of bursts β and the duration of bursts T for simulations of tandem genes. Even in this case we have a good agreement with the results for a single gene. Indeed we find that in the region of higher burst significance we have $\beta \gtrsim 2$ and $T \sim 4 - 5$ min.

For completeness, in Fig. S8 we show the non-Gaussian parameters for the distribution of the supercoiling at the promoter σ_p, already computed for a single gene in the main text. The skewness and the kurtosis are not well-correlated to the burst significance, and the values depend strongly on the particular gene considered in a given configuration. However, for each gene individually, the skewness/kurtosis displays a decreasing/increasing trend as a function of ξ.

In arrays with a pair of divergent genes, the transcription probability for different genes starts to differ as soon as the value of the flux is large enough to give rise to supercoiling mediated interaction (positive feedback loop) between the two divergent genes, Fig. S9a. As a consequence, the burst significance ξ also differs among the genes. Since for high value of the flux ($\bar{J}/D \sim 1$) the transcription across all genes is almost totally dominated by the pair of divergent genes, we find that the latter behave like a single upregulated gene. This can

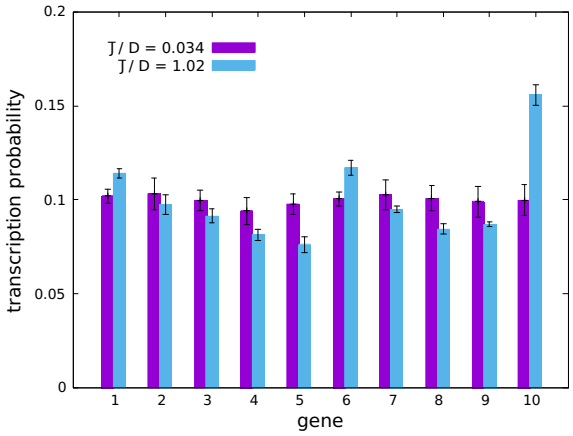

FIG. S6: **Transcriptional probability in the tandem 10-gene array.** The histograms show the transcription probability for each gene, for two different values of the flux, $\bar{J}/D = 0.034$ and $\bar{J}/D = 1.02$, that are the bottom and the top part of the diagram in Fig. 5b in the main text, respectively.

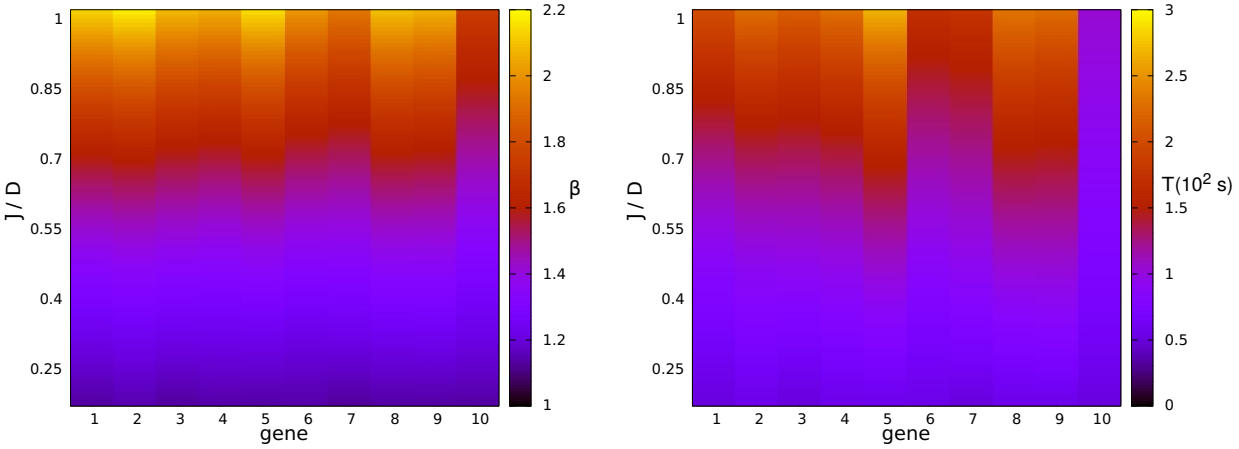

(a) **(b)**

FIG. S7: **Burst size and burst duration in a 10 genes array**. **(a)** Burst size β. **(b)** Burst duration T.

be seen by looking at the distribution of waiting times of one of the two genes (Fig. S9b), which clearly does not display two separate timescales.

As for the tandem setup, we show the burst parameters β and T in the presence of a pair

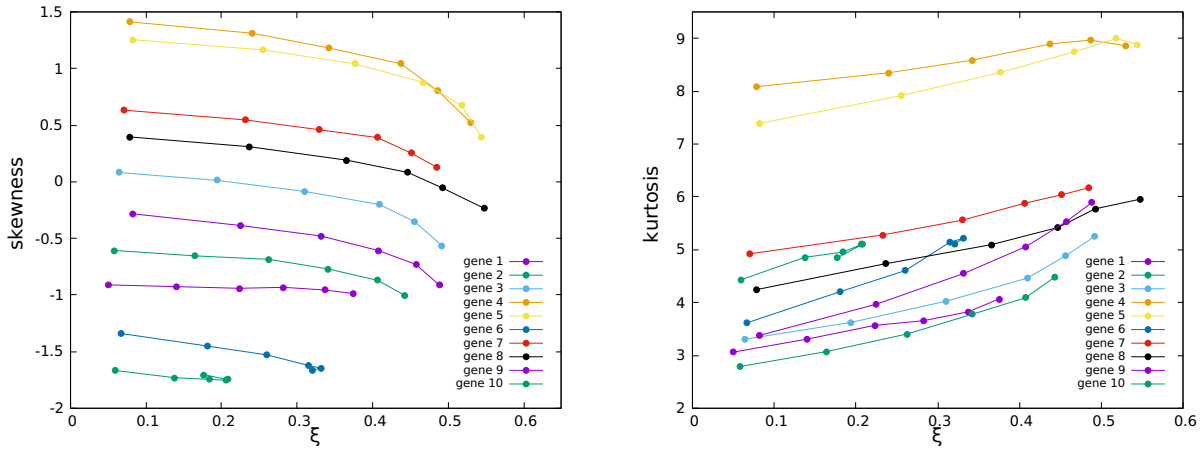

(a) **(b)**

FIG. S8: **Non-Gaussian parameters for simulations with tandem genes**. **(a)** Skewness and **(b)** kurtosis as a function of ξ. For each gene the slowness and the burst significance are computed for different value of the flux $\bar{J}/D$. For each gene the skewness decreases as the bursts significance decreases, whereas the kurtosis increases.

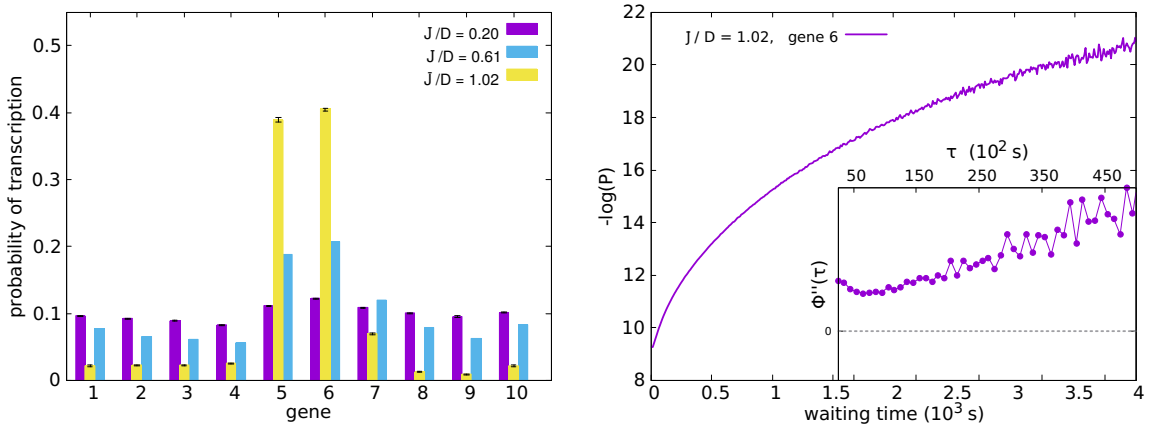

(a) **(b)**

FIG. S9: **Transcription probability and waiting times distribution for gene 6 in a 10 gene array, with a pair of divergent genes**. **(a)** Transcription probability for each gene. For small values of the flux ($\bar{J}/D = 0.2$, purple boxes) genes are almost equally transcribed. As the flux increases, divergent genes start to dominate the dynamics, and their transcription probability increases, while the others are virtually silenced ($\bar{J}/D = 1.02$, yellow boxes). **(b)** Log-linear plot of the waiting time distribution. The system does not display any bistability. Instead, the system visits several states, each of them described by a particular value of supercoiling at the promoter and a corresponding typical waiting time. Inset: the second derivative of $\Phi(\tau)$ does not display zeros, corresponding with the absence of two separate timescales.

of divergent genes (genes 5 and 6, see Fig. S10). We note that the size of bursts is barely greater than 2 for high values of $\bar{J}/D$, since bursty genes are strongly down-regulated.

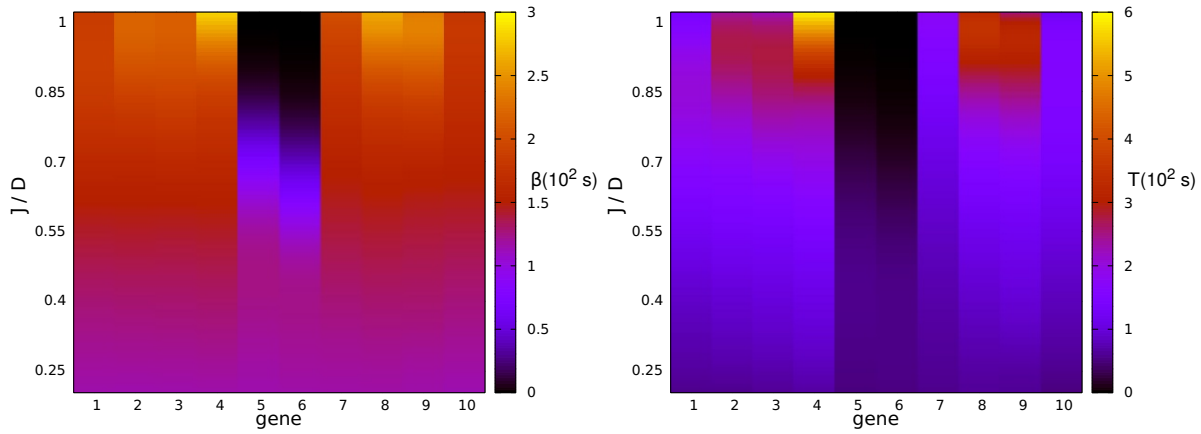

(a) **(b)**

FIG. S10: **Burst size and burst duration in the presence of divergent genes**. **(a)** Burst size β and **(b)** Burst duration T.

[1] C. A. Brackley, J. Johnson, A. Bentivoglio, S. Corless, N. Gilbert, G. Gonnella, and D. Marenduzzo, *Phys. Rev. Lett.*, **117**, 018101 (2016).

[2] M. Dobrzyński, and F. J. Bruggerman, *Proc. Natl. Acad. Sci.*, **106**, 2583 (2009).

[3] N. Kumar, A. Singh, and R. V. Kulkami, *PLoS Comput. Biol.*, **11**, 1004292 (2015).

[4] I. Golding, J. Paulsson, S. M. Zawilski, and E. C. Cox, *Cell*, **123**, 1025 (2005).

[5] S. Chong, C. Chen, H. Ge, and X. S. Xie, *Cell*, **158**, 314 (2014).